CHEMICALLY DEPOSITED THIN-FILM SOLAR CELL MATERIALS

R. Raffaelle, W. Junek
Rochester Institute of Technology, Rochester, NY 14623

J. Gorse, T. Thompson
Baldwin-Wallace College, Berea, OH 44017

J. Harris, D. Hehemann
Kent State University, Kent, OH 44242

A. Hepp, G. Rybicki
NASA Glenn Research Center, Cleveland, OH 44135

Abstract

We have been working on the development of thin film photovoltaic solar cell materials that can be produced entirely by wet chemical methods on low-cost flexible substrates. P-type copper indium diselenide (CIS) absorber layers have been deposited via electrochemical deposition. Similar techniques have also allowed us to incorporate both Ga and S into the CIS structure, in order to increase its optical bandgap. The ability to deposit similar absorber layers with a variety of bandgaps is essential to our efforts to develop a multi-junction thin-film solar cell. Chemical bath deposition methods were used to deposit a cadmium sulfide (CdS) buffer layers on our CIS-based absorber layers. Window contacts were made to these CdS/CIS junctions by the electrodeposition of zinc oxide (ZnO). Structural and elemental determinations of the individual ZnO, CdS and CIS-based films via transmission spectroscopy, x-ray diffraction, x-ray photoelectron spectroscopy and energy dispersive spectroscopy will be presented. The electrical characterization of the resulting devices will be discussed.

1. Introduction

The development of light-weight and efficient photovoltaic solar cells for use in space power applications is of great interest to NASA. It is desirable that these cells should be flexible for easy deployment and control. The materials used in making these cells must also have a good tolerance to the types of radiation they will be exposed to in space. Thin-film solar cells based on copper indium diselenide or CIS have proven to be an excellent candidate for such applications.[1] Wet-chemical methods of producing photovoltaic thin films have also generated much interest. These methods are cost-effective, easily scalable, and can be used to deposit thin-films at low-temperatures on inexpensive flexible substrates.

We have been investigating the use of electrochemically deposited p-type $CuInSe_2$ (CIS) thin films for use as solar cell absorber layers. CIS is an excellent optical absorber with good electrical conductivity.[3] CIS has an optical bandgap of around 1.1 eV, which although not ideal, can be improved by the substitutional doping of Ga for In and/or S for Se.[4] The most efficient thin film solar cells developed to date employ $CuIn_{1-x}Ga_xSe_2$ (CIGS) absorber layers.[5] To produce flexible cells, we have focussed on the growth of CIS-based films on thin Mo foils, and Mo on Kapton.™

The most commonly used window materials for CIS-based solar cells are cadmium sulfide (CdS) and zinc oxide (ZnO) (see Figure 1). The CdS serves as a n-type buffer layer. CdS is well-lattice matched to CIS with a good optical transparency and optical bandgap of approximately 2.4 eV.[6] The CdS films are most commonly deposited using a chemical bath deposition technique.[7] Zinc oxide (ZnO) is a transparent conducting

oxide which serves as the top contact for the cell. ZnO has an optical bandgap of around 3.3 eV and conductivity as high as 200 $\Omega^{-1}cm^{-1}$.[8] Electrochemical deposition and chemical bath deposition techniques have both been previously used to deposit ZnO thin films.[9-10]

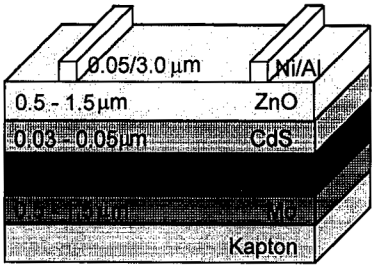

Figure 1. Typical thin-film photovoltaic solar cell.

2. Experimental Details

$CuInSe_2$ was electrochemically deposited on Mo foil, Mo coated Kapton, and indium tin oxide (ITO) coated glass from a solution containing 1 mM $CuSO_4$, 10 mM $In_2(SO_4)_3$, 5 mM SeO_2, 25 mM citric acid, and 10% ethanol by volume. The films were deposited at room temperature using a deposition potential of –1.2 V versus a saturated calomel electrode (SCE). The substrates were mounted in a rotating disk electrode and rotated at 500 r.p.m. The active electrode area had a radius of 1.27 cm. In order to deposit a 1 μm thick film, a deposition time of 600 s was used. The as-deposited films were then annealed in a flowing Argon atmosphere at 400 °C for 1 hour. Thiourea (5 mM) was added to the basic CIS solution as the sulfur source to deposit $CuIn(S,Se)_2$ films. To deposit $Cu(In,Ga)Se_2$, a $CuGa_2$ film was first electrodeposited at –1.8 V vs. SCE for 300 s from a 1 mM $Cu(SO_4)$, 20 mM $Ga_2(SO_4)_3$, and 5 M NaOH bath, before depositing the CIS. These resulting films were annealed at 600°C for 1 hour in flowing argon.

CdS buffer layers were grown on the CIS-based absorber layers using chemical bath deposition. The CIS-based films were immersed for 600 s in a 60 °C solution of 1mM Cd-acetate, 1 M NaOH, and 60 mM thiourea. The top contacts were made by electrochemical deposition of ZnO at –1.0 V vs. SCE for 300 s using a solution of 100 mM $Zn(NO_3)_2$ in deionized water held at 60 °C.

X-ray diffraction was performed on each of the deposited films associated with this study using a Phillips PW 3710 diffractometer. The surface morphology of the films were examined in a Hitachi S-4700 FE-SEM. Energy dispersive spectroscopy was also performed in the SEM using an EDAX DX prime system utilizing ZAF standardless correction. X-ray photoelectron spectroscopy was used in conjunction with argon ion ablation to depth profile the CIS deposited on Mo. Sensitivity factors based on the EDS results were used to quantify the measurements.

Transmission spectrophotometry was performed on the films deposited on ITO coated glass using a Perkin Elmer Lamba 19 spectrophotometer. This data was converted to absorption coefficients using the film thickness as determined by a Dektak II profilometer. The resulting absorption coefficients versus photon energy plots were used to determine the optical bandgaps of the films.

An Alessi four-point probe was used to monitor the conductivity of the different films deposited in this study. The four-point probe was also used to type the different semiconductors deposited via the Seebeck effect.

Current versus voltage measurements on the ZnO/CdS/CIS junctions were performed using a computer controlled Keithley 236 source/measure unit. Contacts were made to the device using silver paint and an Alessi Rel-2100 wafer probing station.

3. Results and Discussion

The SEM micrographs of the $CuInSe_2$ $CuIn(S,Se)_2$, and $CuInS_2$ films which were electrodeposited at –1.2 V vs. an SCE on Mo foil are shown in Figure 2. The samples show increasing roughness with sulfur incorporation. This behavior is most probably due to the volatility of the sulfur during the annealing process. The films were all conducting and p-type as determined by the polarity of the Seebeck voltage using a four-point probe.

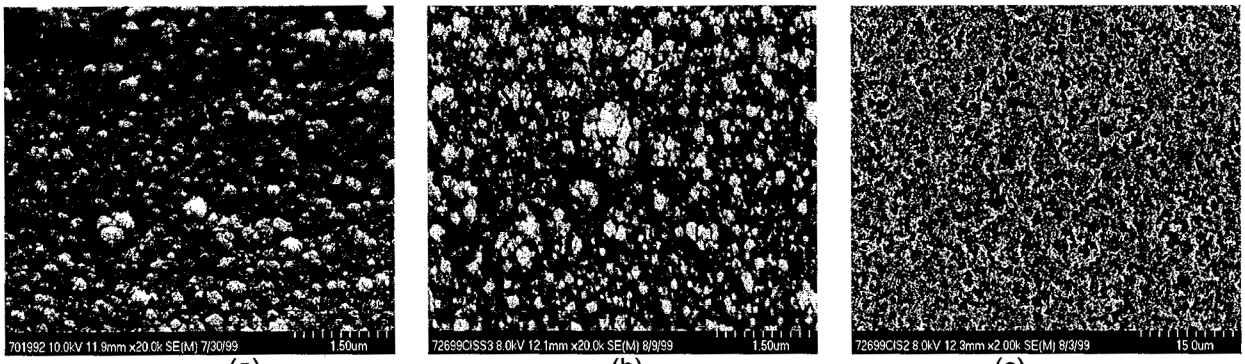

Figure 2. SEM micrographs of electrodeposited (a) $CuInSe_2$, (b) $CuIn(Se,S)_2$, (c) $CuInS_2$.

X-ray photoelectron spectroscopy (XPS), in conjunction with argon ion ablation, was used to depth profile a CIS on Mo film. Energy dispersive spectroscopy (EDS) was used to determine the bulk atomic ratios. These results were used to identify the sensitivity factors used in the XPS measurement. The EDS results showed that the CIS deposited at –1.2 V vs. SCE is copper rich ([Cu]=28%, [In]=22%, [Se]=50%). The XPS profile of the same film indicates that it had a uniform composition in the direction perpendicular to the substrate (see Figure 3). The results show a slight increase in the selenium concentration and a decrease in the copper concentration at the surface of the sample.

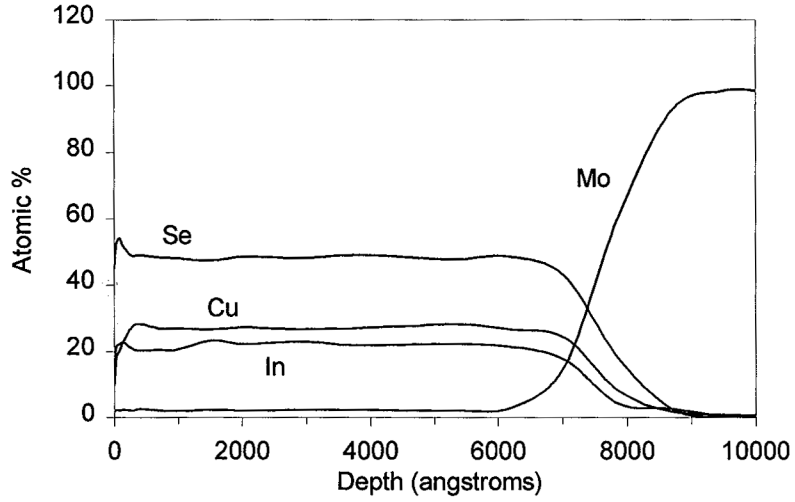

Figure 3. XPS depth profile of a CIS thin film deposited at –1.2 V vs. SCE for 600 s and annealed at 400 °C for 1 hour in flowing argon.

X-ray diffraction (XRD) of the CIS-based absorber films confirmed that they all had the basic chalcopyrite crystal structure. A shift is seen in the main Bragg peaks as either Ga or S is introduced into the CIS lattice. Figure 4 shows a comparison of the XRD pattern for a CIGS film to the reference patterns for $CuInSe_2$ and $CuIn_{0.5}Ga_{0.5}Se_2$. Figure 5 shows a comparison of the XRD pattern of a $CuIn(Se,S)_2$ film to the reference patterns of $CuInSe_2$, $CuIn(Se_{0.5},S_{0.5})_2$, and $CuInS_2$. These results indicate that both Ga and/or S are being incorporated into the basic CIS structure. XRD results also confirmed that the CdS films had a hexagonal crystal structure and the ZnO was in the zincite structure.

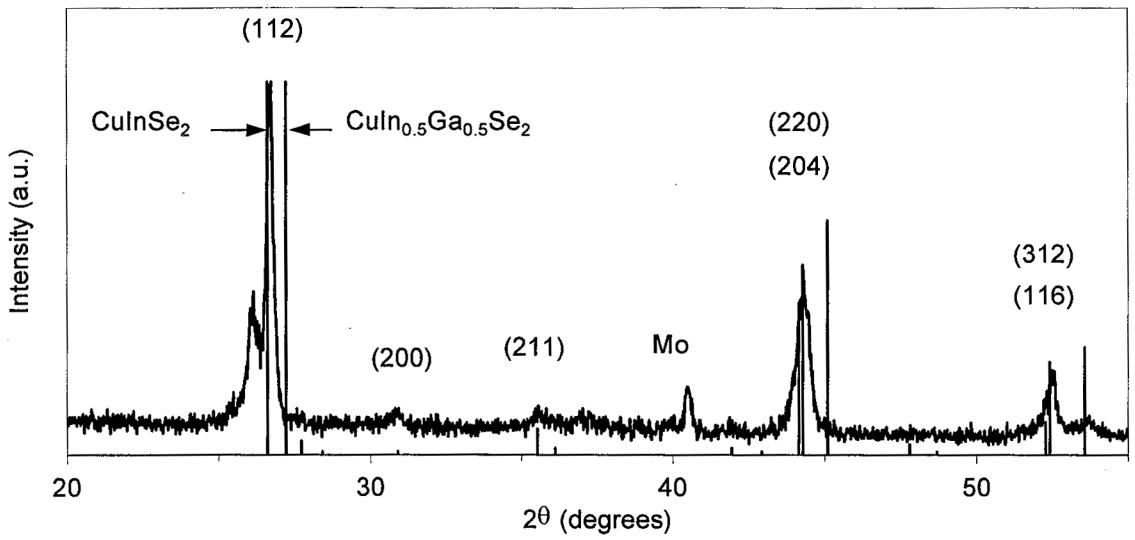

Figure 4. XRD pattern of Ga-doped CIS overlayed on $CuInSe_2$ and $CuIn_{0.5}Ga_{0.5}Se_2$ reference patterns.

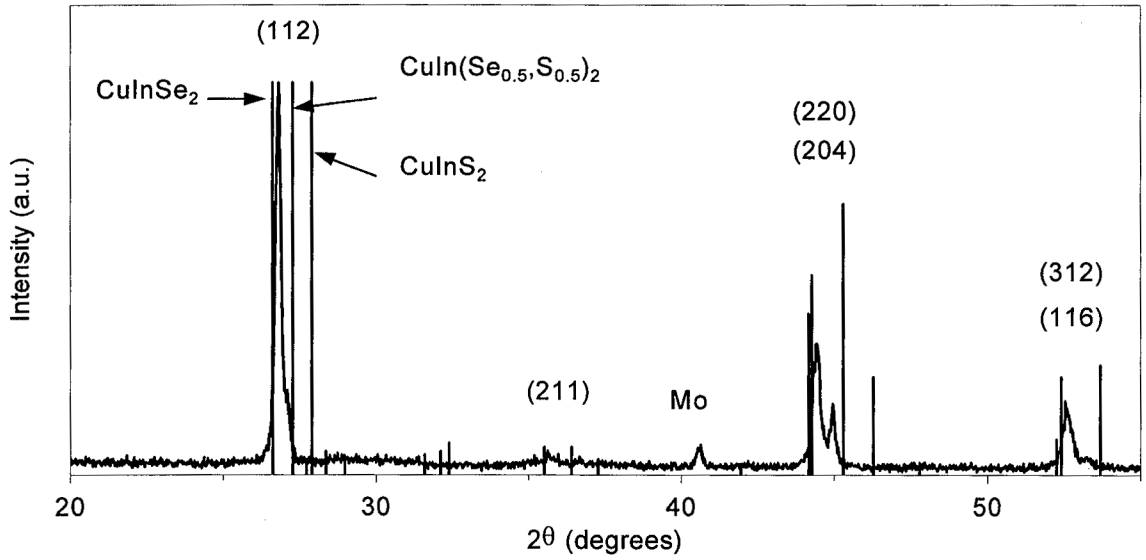

Figure 5. XRD pattern of S-doped CIS overlayed on $CuInSe_2$, $CuIn(Se_{0.5},S_{0.5})_2$, and $CuInS_2$ reference patterns.

We used optical transmisson spectroscopy to determine the optical bandgaps for the absorber and window films. The raw transmission data was coverted to absorption coefficients after film thickness was determined using a Dektak II profilometer. The absorption coeffcients were then used to determine the optical bandgaps, assuming the direct bandgap relation

$$\alpha = \frac{\left(E_g - h\upsilon\right)^{1/2}}{h\upsilon} \tag{1}$$

The CdS, ZnO, and CIS-based films deposited on ITO coated glass showed good linearity when plotted in accordance with Eq. 1, indicating that they are direct bandgap semiconductors. The optical bandgaps were determined from the x-intercepts of a least-squares fit to the linear portion of the curves (see Figure 6). The

values of 1.1 eV, 2.4 eV, and 3.3 eV for CIS, CdS, and ZnO, respectively are in good agreement with their accepted values.[4,6,8] A shift to larger values was also verified for S incorporation into $CuInSe_2$ (see Figure 7).

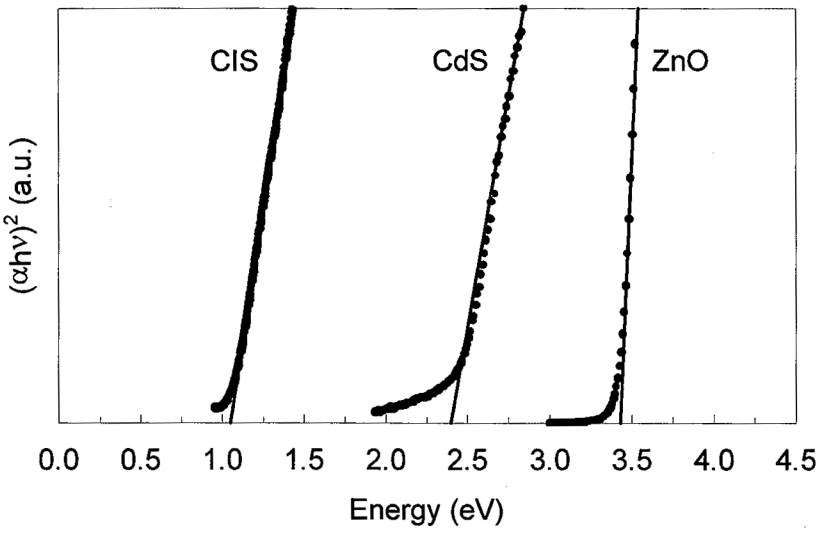

Figure 6. Optical bandgaps for $CuInSe_2$, CdS, and ZnO. The y-values have been normalized and plotted in arbitrary units in order to display the different materials on the same plot.

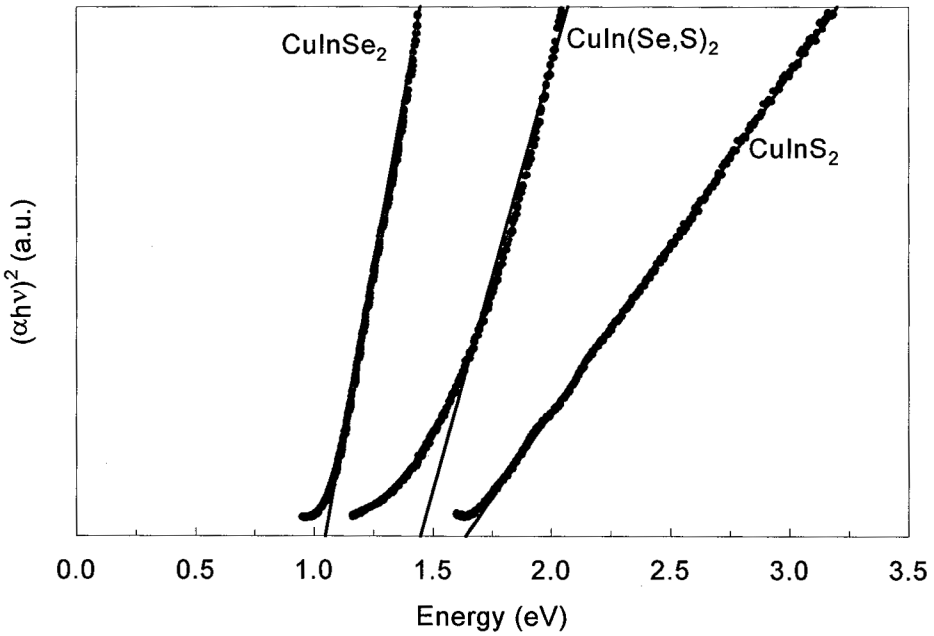

Figure 7. Optical bandgaps for $CuInSe_2$, $CuIn(Se,S)_2$, and $CuInS_2$. The y-values have been normalized and plotted in arbitrary units in order to display the different materials on the same plot.

The current versus voltage behavior of a device that consisted of electrodeposited ZnO on chemical bath deposited CdS, on electrodeposited $CuInSe_2$, on thin Mo foil, is shown in Figure 8. The device exhibited good rectification with a measurable short-circuit photo-current under ambient lighting. However, the device had an open-circuit voltage of only 220 mV and considerable reverse-bias leakage current. These results are most

likely attributable to point defects near the junction and/or grain boundary shunting. Improvement in the junction performance is being addressed by changes in the absorber stoichiometry and improved annealing conditions. The shallow slope of the forward-bias current versus voltage behavior indicates a significant series resistance. This resistance is probably a result of poor conductivity in the top contact. The top contact performance is being studied as a function of the deposition voltage and temperature of the ZnO. Improvement through the use of a post-deposition annealing of the ZnO is also being examined.

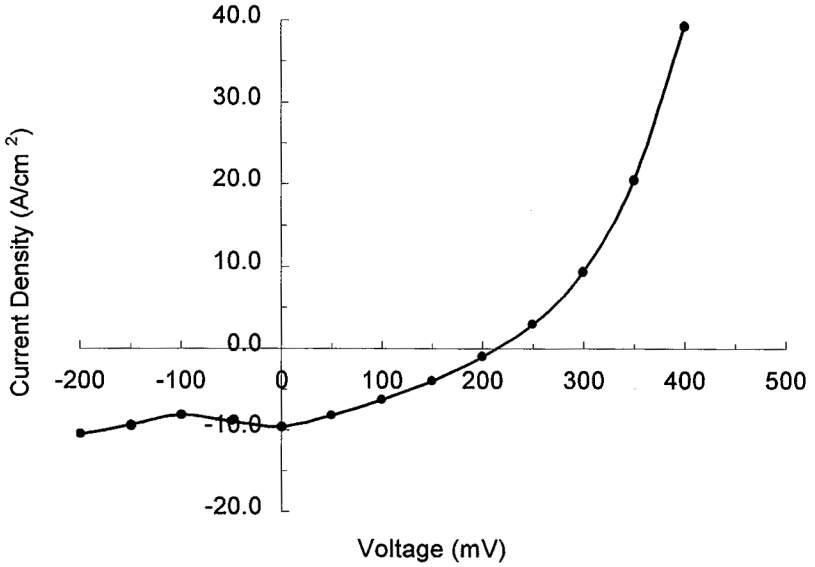

Figure 8. Current versus voltage characteristics of a ZnO/CdS/CIS solar cell under ambient light.

4. Conclusions

Compositionally uniform p-type $CuInSe_2$ thin films were deposited on inexpensive flexible substrates using low-temperature electrochemical deposition. X-ray diffraction analysis confirmed that it is possible to sustitutionally dope Ga and S for In and Se, repectively in $CuInSe_2$ thin films using electrochemical deposition. Optical spectroscopy verified that the incorporation of S into $CuInSe_2$ signifcantly increased the optical bandgap of the materials. Low-temperature electrochemical depostition and chemical bath deposition were used to deposit ZnO transparent conductive windows and CdS buffer layers, respectively onto p-type $CuInSe_2$. This combination of electrochemical and chemical bath deposition techniques were succesfully used to produce a working heterojunction thin-film photovoltaic solar cell.

5. References

[1] D.J. Flood, *Int'l Photovolt. Solar Energy Conf.*, **5**, Japan (1990) 551.
[2] C. Guillen and J. Herrero Sol. *Energy Mater. And Sol. Cells*, **43** (1996) 47.
[3] K. Zweibel, H.S. Ullal, and B. von Roedem, *25th IEEE Photovoltaic Specialists Conf.*, (IEEE, Washington, 1996) 159.
[4] H.W. Schock, *Solar Energy Materials and Solar Cells* **34** (1994) 19.
[5] J.R. Tuttle, M.A. Contreras, T.J. Gillispie, K.R. Ramanathan, A.L. Tenant, J. Keane, A.M. Gabor, and R, Noufi, *Prog. Photovoltaics* **3** (1995) 235.
[6] R.W. Birkmire, B.E. McCandless, W.N. Shafarman, and R.D. Varrin, *Proc. Of the 9th European Photovoltaic Solar Energy Conference*, Freiburg, Germany (Kluwer Academic Publishers, Dodrecht, 1991) 1415.
[7] B.R. Lanning and J.H. Armstrong, *Int. J. Solar Energy* **12** (1992) 247.
[8] J. Ma, F. Ji, H. Ma, S. Li, *Thin Solid Films* **279** (1996) 213.
[9] J. Lee and Y. Tak, *Mat. Res. Soc. Symp.* **495** (1998) 457.
[10] K. Ito and K. Nakamura, *Thin Solid Films* **286** (1996) 35.